Glassy carbon electrode modified with 7,7,8,8-tetracyanoquinodimethane and graphene oxide triggered a synergistic effect：low-potential amperometric detection of reduced glutathione

Baiqing Yuan [a, *], Chunying Xu [a], Renchun Zhang [a], Donghui Lv [a], Sujuan Li [a], Daojun Zhang [a], Lin Liu [a], Carlos Fernandez [b, *]

[a] Henan Province Key Laboratory of New Optoelectronic Functional Materials, College of Chemistry and Chemical Engineering, Anyang Normal University, Anyang 455000, Henan, China

[b] School of Pharmacy and Life Sciences, Robert Gordon University, Garthdee Road, Aberdeen AB10 7GJ, United Kingdom.

* Corresponding author.

E-mail: baiqingyuan1981@126.com (B. Yuan); c.fernandez@rgu.ac.uk (C. Fernandez)

1

Abstract

A sensitive electrochemical sensor based on the synergistic effect of 7,7,8,8-tetracyanoquinodimethane (TCNQ) and graphene oxide (GO) for low-potential amperometric detection of reduced glutathione (GSH) in pH 7.2 phosphate buffer solution (PBS) has been reported. This is the first time that the combination of GO and TCNQ have been successfully employed to construct an electrochemical sensor for the detection of glutathione. The surface of the glassy carbon electrode (GCE) was modified by a drop casting using TCNQ and GO. Cyclic voltammetric measurements showed that TCNQ and GO triggered a synergistic effect and exhibited an unexpected electrocatalytic activity towards GSH oxidation, compared to GCE modified with only GO, TCNQ or TCNQ/electrochemically reduced GO. Three oxidation waves for GSH were found at -0.05, 0.1 and 0.5 V, respectively. Amperometric techniques were employed to detect GSH sensitively using a GCE modified with TCNQ/GO at -0.05 V. The electrochemical sensor showed a wide linear range from 0.25 to 124.3 μM and 124.3 μM to 1.67 mM with a limit of detection of 0.15 μM. The electroanalytical sensor was successfully applied towards the detection of GSH in an eye drop solution.

1. Introduction

Glutathione (GSH, γ-glutamyl-L-cysteinyl-glycine), the most abundant tripeptide thiol in eukaryotic and mammalian cells, performs a high number of physiological roles including protection against natrosative and oxidative stress (Areias et al., 2016). GSH has been found in both mammalian and plant tissue over the concentration range from 1 to 10 mM (Valero-Ruiz et al., 2016), and its levels are an indicator of various diseases such as HIV, cancer, Alzheimer's disease, and diabetes (Harfield et al., 2012). Therefore, developing sensitive and selective methods for GSH detection has attracted a lot of attention for medical diagnosis.

Electrochemcal determication of GSH is gaining momentum among other analytical methods due to its simplicity, high sensitivity, low cost and fast analysis (Harfield et al., 2012). The electrochemical oxidation of GSH at bare GCE requires high overpotential. As a result, various electrocatalysts have been utilized either modified on the electrode surface or placed in solution as a mediator to decrease the overpotential of GSH. The reported modification materials and mediators found in literature are thoroughly reviewed in **Table 1**. The electrochemical techniques most commonly employed are differential pulse voltammetry (DPV) and amperometric detection. However, a key problem with the analysis of GSH utilizing DPV is that the voltammetric peak resulting from the electrochemical oxidation of GSH may overlap with the electroactive coexisting species such as ascobic acid (AA), uric acid (UA), dopamine (DA) and cysteine (CYS). When amperometric detection is employed, the oxidation potential of GSH is required to be much lower than these coexisting species

3

67   to prevent their interference.

68   7,7,8,8-Tetracyanoquinodimethane (TCNQ) is an effective electron transfer

69   mediator due to the presence of four cyano groups and π conjugation bonds, which

70   can form organic charge-transfer complexes and ion-radical salts such as K (TCNQ)

71   and Na (TCNQ) (Zamfir, et al., 2013; Paczosa-Bator et al., 2015). In addition, TCNQ

72   has attracted considerable interest in the fabrication of electrochemical sensors for

73   carbamate drugs (Zamfir, et al., 2013), K^+ (Paczosa-Bator et al., 2015),

74   acetylcholinesterase inhibitors (Rotariu et al., 2012) and ascobic acid (Murthy and

75   Anita, 1994). GO is a highly oxidized derivative of graphene, which possesses a large

76   amount of oxygen functional groups such as hydroxyl, epoxide, carboxyl, and

77   carbonyl groups (Zhu et al., 2010). The oxygen functional groups can increase the

78   charge transfer resistance, but play an essential role in the electrocatalytic oxidation of

79   some small molecules including AA (Uhma et al., 2011), DA (Xiong and Jin, 2011),

80   dihydroxybenzene isomers, and L-methionine (Zhang et al., 2014). To the best of our

81   knowledge, we have reported for the first time the fabrication of an electrochemical

82   sensor using GCE modified with TCNQ and GO for the detection of GSH. In addition,

83   the modified GCE sensor with TCNQ/GO showed an unexpected electrocatalytic

84   activity towards GSH oxidation at a low potential compared to electrodes modified

85   with only GO, TCNQ and TCNQ/electrochemically reduced GO (rGO). Furthermore,

86   TCNQ and GO also showed a synergistic effect on the electrocatalytic oxidation of

87   GSH with the oxidation overpotential decreasing greatly. Finally, based on the

88   TCNQ/GO/GCE electrode, sensitive amperometric determination of GSH was

4

89   successfully achieved.

2. Experimental

2.1. Chemicals and solutions

TCNQ, GSH, CYS, DA, AA, and UA were purchased from Sigma-Aldrich. GO was acquired from Nanjing XFNano Materials Tech Co., Ltd. All other chemicals were of analytical reagent grade, and doubly distilled water was used to prepare all the solutions. 0.1 M phosphate buffer solution (PBS, pH 7.2) was employed as the background electrolyte.

2.2. Apparatus

Scanning electron microscopy (SEM) images were obtained with a Hitachi SU8010 (Japan) scanning electron microscope. A CHI 842C electrochemical workstation (Austin, TX, USA) was used to perform all the electrochemical experiments with a conventional three-electrode system, which included a GCE as the working electrode, a platinum coil as an auxiliary electrode, and an Ag/AgCl (saturated KCl) as the reference electrode.

2.3. Electrode preparation and modification

Prior to each experiment, GCE with a geometric area of 0.07 cm^2 was polished with 1, 0.3, and 0.05 μm alumina paste to a mirror finish, subsequently, the electrode was rinsed with water, and finally an ultrasonic treatment in water and ethanol was applied, respectively. GO modified GCE was prepared by droping a 5 μL of 1 mg/mL GO aqueous solution on the cleaned electrode and kept to dry at room temperature. Due to the low surface tension of acetone solution, TCNQ modified electrodes were prepared

111   by a drop casting method via solvent evaporation (Nafady et al., 2006). Briefly, the

112   GO modified GCE or bare GCE was dipped in a 10 mM fresh solution of TCNQ in

113   acetone for one minute and then kept in air to dry face down. To fabricate rGO

114   modified GCE, firstly, the GO/GCE was electrochemically reduced in pH 4.0 acetate

115   buffer by amperometric method for 500 s at -1.2 V, then the electrode was modified

116   with TCNQ using the similar method as TCNQ/GO/GCE. The electroactive surface

117   areas of these electrodes could be calculated by the Randles–Sevcik equation

118   (Supplementary information).

119   **3. Results and discussion**

120   *3.1. SEM Characterization of TCNQ modified electrodes*

121   The electrode surface characterization was analyzed by SEM. **Fig. 1** shows the

122   SEM images of TCNQ modified electrode by a drop casting method. As shown in **Fig.**

123   **1D, E, and F**, irregular TCNQ plates erected on the surface of GCE without GO due

124   to gravity. However, in the presence of GO, rhombic TCNQ plates structures were

125   formed and lay on the surface of GO/GCE (**Fig. 1A, B, and C**), those structures

126   formation were attributed to the π-π interaction between GO and TCNQ. The size of

127   the formed TCNQ crystals were found to be over the range from 5 to 30 μm.

128   *3.2. Electrochemical properties of TCNQ modified electrodes*

129   Next, the electrochemical properties of TCNQ modified electrodes were

130   investigated. TCNQ exhibits two electrochemically reversible one-electron waves,

131   which were associated to the generation of $TCNQ^{\cdot-}$ and $TCNQ^{2-}$ by using the

132   following equations:

133        $TCNQ + e^- = TCNQ \cdot^-$ (1)

134        $TCNQ \cdot^- + e^- = TCNQ^{2-}$ (2)
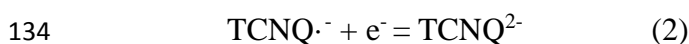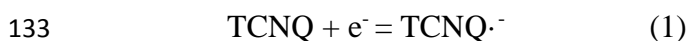
135   **Fig. 2A** *Inset* shows the CVs of TCNQ immobilized on GCE by a drop casting

136   method in 0.1 M pH 7.2 PBS. It can be seen that a pair of typical redox peaks

137   appeared at 0.5 and -0.15 V, respectively. Surface-immobilized TCNQ also undergoes

138   a remarkable 'inert zone' in which no faradaic reaction yields, suggesting a typical

139   solid-solid phase transformation in terms of nucleation and growth (Gómez and

140   Rodríguez-Amaro, 2006). Further, with the increasing cycle, the voltammetric peak

141   heights decay due to the dissolution of TCNQ into the solution (Bond et al., 1998).

142   The results obtained are in good agreement with previous reports (Gómez and

143   Rodríguez-Amaro, 2006; Bond et al., 1998). The electrochemical behaviour of

144   immobilized TCNQ on the surface of GO or rGO was also studied, as shown in **Fig.**

145   **2B and C** *Inset*. Both CVs differ considerably from that obtained at TCNQ/GCE. The

146   electrochemical processes at the GCE modified with TCNQ/GO showed three pairs of

147   redox waves (**Fig. 2B** *Inset*). According to Eqs. (1) and (2), the two corresponding

148   oxidation peak potentials were observed at -0.05 and 0.36 V, and the corresponding

149   reduction waves appeared at -0.15 and 0.10 V, respectively. The peak 3 showed in Fig.

150   2B Inset is due to the electrochemical behavior of the oxygen functional species on

151   GO, which can also be found in **Fig. 2D** (Yuan et al., 2013c; Ndamanisha et al., 2009)**.**

152   When the GCE was modified with TCNQ/rGO, two electrochemical processes were

153   identified and the corresponding oxidation and reduction waves changed to -0.17 and

154   0.13 V, and -0.32 and 0.05 V, respectively. In addition, the two electrochemical

7

155 processes became much more reversible than that obtained at TCNQ/GO/GCE. This

156 was attributed to the fast electron transfer rate of rGO. The results also showed that

157 the dissolution of TCNQ in solution decreased at the TCNQ/GO/GCE due to the π-π

158 interaction between TCNQ and GO.

159 *3.3. Electrocatalytic oxidation of GSH based on TCNQ modified electrodes*

160 The electrochemical oxidation of GSH using various modified electrode surfaces in

161 0.1 M pH 7.2 PBS by cyclic voltammogram (CV) at a scan rate of 0.1 V/s was also

162 investigated, as shown in **Fig. 2**. When the GCE was modified with GO an oxidation

163 peak was observed at 0.22 V due to the GSH oxidation reaction to GSSG (**Fig. 2D**).

164 This is caused by the electrocatalyic activity of oxygen functional species present on

165 GO towards the oxidation of GSH. The oxidation peak of GSH appeared at 0.7 V

166 when the GCE was modified with TCNQ (**Fig. 2A**). Upon addition of GSH to the

167 solution, three oxidation waves emerged at the TCNQ/GO/GCE with the

168 corresponding oxidation peak potentials of -0.05, 0.1, and 0.5 V, respectively shown

169 in. **Fig. 2B**. These three enhanced oxidation waves were attributed to the

170 electrocatalysis of TCNQ·⁻, oxygen functional groups, and $TCNQ^{2-}$ with the oxidation

171 of GSH. In addition, the catalytic current at 0.1 V is much higher than that obtained at

172 GO/GCE (**Fig. 2D**) with a much lower oxidation potential. The introduction of TCNQ

173 enhanced the electrocatalytic activity of oxygen functional groups present on GO.

174 However, there was no electrocatalytic current observed until 0.35 V when the GCE

175 surface was modified with TCNQ/rGO, even though rGO has high electrical

176 conductivity and fast electron transfer rate. The comparison results showed that

177   TCNQ and GO had a synergistic effect, which exhibited unexpected electrocatalytic

178   activity towards the oxidation of GSH. The electrocatalytic mechanism proposed is

179   shown by equations 3 and 4:

180   $$TCNQ^{\cdot-} + 2GSH = TCNQ + GSSG + 2H^+ \qquad (3)$$

181   $$TCNQ^{2-} + 2GSH = TCNQ + GSSG + 2H^+ \qquad (4)$$

182   The electrochemical detection of GSH in physiological samples had presented a major

183   obstacle due to the presence of electroactive species such as AA, DA, UA, and CYS

184   which often coexists with GSH. The ultra-low overpotential of GSH shown at the

185   TCNQ/GO/GCE may overcome the interferences from these interfering species. Next,

186   the selectivity of the proposed electrochemical sensor (modified GCE with TCNQ/GO)

187   was investigated by CV. **Fig. 3** shows the CVs of TCNQ/GO/GCE in the absence

188   (dotted line) and presence (solid line) of 0.2 mM AA (A), 5 mM CYS (B), 0.2 mM

189   DA (C), and 0.2 mM UA (D) in 0.1 M 7.2 pH PBS at a scan rate of 0.1 V/s. The

190   oxidation peak for UA was found to be at 0.38 V, which is much higher than the first

191   and second oxidation wave of GSH because of the ultra-low overpotential of GSH at

192   the TCNQ/GO/GCE. Two pairs of redox peaks were observed for DA. Further

193   experiments indicated that the first oxidation process for DA at 0.23 V is essential to

194   form the second oxidation. Therefore, the oxidation potential of DA is also higher

195   than the first two oxidation waves of GSH. AA and CYS had a similar electrocatalytic

196   oxidation as GSH, but the electrocatalytic current is lower than that of GSH. It was

197   reported that the concentration of GSH in the cells can be up to 10 mM (Mesiter,

198   1988), while the basal level of AA in the extracellular fluid of the central nervous

9

199 system, is approximately 0.1 μM, and the physiological level of AA is about 0.1 mM

200 (El-Said et al., 2010). Considering the far higher level of GSH compared to AA in

201 physiological samples and high sensitivity for GSH detection of this method, the

202 influence of AA may be decreased and even ignored by diluting the sample. In

203 addition, AA can be removed from the sample by adding ascorbate oxidase (Silva, et

204 al. 2013) before analysis. Therefore, it is possible to apply the mthod for the detection

205 of GSH in biological fluids.

206 *3.4. Amperometric sensing of GSH based on a GCE modified with TCNQ/GO*

207 Next, we investigate the electrochemical detection of GSH on a GCE modified with

208 TCNQ/GO using amperometric techniques. **Fig. 4** shows the amperometric response

209 of TCNQ/GO/GCE to the successive additions of GSH in a stirring pH 7.2 PBS

210 solution. Due to the high electrocatalytic activity of the TCNQ/GO/GCE towards the

211 GSH oxidation, much lower potentials (-0.05 or 0.1 V) were used. For -0.05 V and 0.1

212 V amperometric sensing, the measured current increased with the GSH concentrations,

213 and a linear response was observed over a concentration range of 0.25-124.3 μM

214 (R^2=0.9928, I/μA=0.029+2.09 C/mM) and 124.3 μM-1.67 mM (R^2 =0.9989,

215 I/μA=0.37+0.35 C/mM), and 0.25-174.3 μM (R^2=0.9956, I/μA=0.37+0.34 C/mM)

216 and 174.3 μM-1.18 mM, (R^2=0.9972, I/μA=0.50+0.78 C/mM), respectively. The limit

217 of detection was calculated to be 0.15 μM and 0.10 μM (S/N=3), respectively. The

218 analytical performance of GSH with the GCE modified with TCNQ/GO reported in

219 this work and other modified materials and mediators found in literature are

220 thoroughly reviewed in **Table 1**. The oxidation potential of GSH at the

221 TCNQ/GO/GCE (-0.05 V) is much lower than those other materials or mediators but

222 higher than catechol (-0.16 V) illustrated in Table 1. The TCNQ/GO/GCE also

223 displayed a wide linear range for the detection of GSH compared to other electrodes.

224 It should be noted that, with the addition of high GSH concentrations, the

225 amperometric responses decreased with time, suggesting that further GSH oxidation

226 was greatly hindered. This may be caused by the passivation of electrode due to the

227 binding of the sulfur moiety to the electrode surface generated by the oxidation of

228 GSH because the concentration of GSH reached a high level in the detection cell with

229 the successive additions of GSH (Harfield, et al., 2012). The similar phenomenon was

230 also reported in the previous literature (Yuan, et al., 2013c).

231 In order to assess the anti-interference performance of TCNQ/GO/GCE, the

232 interference effect was also examined at the TCNQ/GO/GCE with 25 μM GSH in the

233 presence of 4 μM AA, 4 μM CYS, 25 μM DA, and 25 μM UA by using amperometric

234 technique (Supplementary information). The results showed that the presence of these

235 electroactive species with the added concentration did not interfere with the

236 determination of GSH due to the low detection potential at which was applied. This is

237 also in agreement with the interference test by CV method in section 3.3.

238 The stability of the electrochemical sensor was investigated by a continuous

239 operation and successive performance. After 2300 s of continuous operation of 25 μM

240 GSH, 98% of its initial value was retained (Supplementary information). After being

241 stored in air for one week and two weeks, respectively, the electrode had a 12% and

242 18% decrease in current response (Supplementary information). In addition, the RSD

11

243 was 4.7% for ten successive analysis of 25 µM GSH using the same electrode. This

244 excellent stability of the presented sensor was due to the π-π interaction between GO

245 and TCNQ.

246 *3.5. Analysis of GSH in real samples*

247 The applicability of the sensor was further evaluated by the analysis of GSH in an

248 eye drop solution (purchased from Wuhan Wujing Medicine Co., Ltd, China). 2.0 µL

249 sample without pretreatment was directly added to a stirring PBS solution at pH 7.2

250 (8.0 mL) for amperometric detection. The GSH concentration in the eye drops

251 solution was found to be 60.8 mM, which is in agreement with the labeled value (65.0

252 mM). The recoveries were also estimated by adding GSH standards to the above

253 solution. The results showed that the sensor gave the acceptable recoveries over the

254 range between 94.7% and 106.1%.

255 **4. Conclusions**

256 A simple TCNQ and GO modified GCE was prepared and used for the

257 electrocatalytic oxidation of GSH at physiological pH. The results showed that TCNQ

258 and GO triggered an outstanding synergistic effect which enhanced the

259 electrocatalytic activity towards the oxidation of GSH. As a result, the oxidation

260 potential of GSH decreased to an ultra-low value (-0.05 V). Based on the TCNQ and

261 GO modified GCE, low potential amperometric detection of GSH was achieved with

262 wide linear range and low detection limit. The electrochemical protocol was

263 successfully applied towards the detection of GSH in a real sample (eye drop solution)

264 with a recovery from 94.7 to 106.1%. As an effective electrocatalysts, the TCNQ and

12

265 GO opens a new potential application in biosensing.

266 **Acknowledgments**

274

275

276

277

278

279

280

281

282

283

284

285

286

287 **References**

288 Areias, M.C.C., Shimizu, K., Compton, R.G., 2016. Analyst 141, 2904–2910.

289 Atta, N.F., Galal, A., Azab, S.M., 2012. Anal. Bioanal. Chem. 404, 1661–1672.

290 Bond, A.M. Fletcher, S., Symons, P.G., 1998. Analyst 123, 1891–1904.

291 Chatraei, F., Zare, H.R., 2011. Analyst 136, 4595–4602.

292 Chee, S.Y., Flegel, M., Pumera, M., 2011. Electrochem. Commun. 13, 963–965.

293 El-Said, W.A., Lee, J.H., Oh, B.K., Choi, J.W., 2010. Electrochem. Commun. 12,

294   1756–1759.

295 Ensafi, A.A. Karimi-Malehb, H. Mallakpour, S., 2013. Colloids Surf. B 104, 186–193.

296 Eremenko, A.V., Dontsova, E.A., Nazarov, A.P., Evtushenko, E.G., Amitonov, S.V.,

297   Savilov, S.V., Martynova, L.F., Lunin, V.V., Kurochkin, I.N., 2012. Electroanal.

298   24, 573–580.

299 Gómez, L., Rodríguez-Amaro, R., 2006. Langmuir 22, 7431–7436.

300 Harfield, J.C., Batchelor-McAuley, C., Compton, R.G., 2012. Analyst 137,

301   2285–2296.

302 He, H., Du, J., Hu, Y., Ru, J., Lu, X., 2013. Talanta 115, 381–385.

303 Hosseini, H., Ahmar, H., Dehghani, A., Bagheri, A., Tadjarodi, A., Fakhari, A.R.,

304   2013. Biosens. Bioelectron. 42, 426–429.

305 Hou, Y., Ndamanisha, J.C., Guo, L., Peng, X., Bai, J., 2009. Electrochim. Acta 54,

306   6166–6171.

307 Huang, Y., Yan, H., Tong, Y., 2015. J. Electroanal. Chem. 743, 25–30.

308 Inoue, T., Kirchhoff, J.R., 2000. Anal. Chem. 72, 5755–5760.

309   Karimi-Maleh, H., Tahernejad-Javazmi, F., Ensafi, A., Moradi, R., Mallakpour, S.,

310   Beitollahi, H., 2014. Biosens. Bioelectron. 60, 1–7.

311   Lee, P.T., Goncalves, L.M., Compton, R.G., 2015. Sens. Actuators B: Chem. 221,

312   962–968.

313   Li, X., Zheng, L., Wang, Y., Zhang, N., Lou, Y.   Xiao, T. Liu, J., 2015. RSC Adv. 5,

314   71749–71755.

315   Liu, B., Wang, M., Xiao, B., 2015. J. Electroanal. Chem. 757, 198–202.

316   Luz, R.C.S., Damos, F.S., Tanaka, A.A., Kubot, L.T., Gushikem, Y., 2008. Talanta 76,

317   1097–1104.

318   Medina-Ramos, J., Oyesanya, O., Alvarez, J.C., 2013. J. Phys. Chem. C 117,

319   902−912.

320   Mesiter, A., 1988. J. Bio. Chem. 263, 17205−17208.

321   Mu, S., Yang, Y., 2016. J. Electroanal. Chem. 780, 12–18.

322   Murthy, A.S.N., Anita, 1994. Biosens. Bioelectron. 9, 439–444

323   Narang, J., Chauhan, N., Jain, P., Pundir, C.S., 2012. Int. J. Biol. Macromol. 50,

324   672–678.

325   Ndamanisha, J.C., Bai, J., Qi, B., Guo L., 2009. Anal. Biochem. 386, 79–84.

326   Nafady, A., O'Mullane, A.P., Bond, A.M. Neufeld, A.K., 2006. Chem. Mater. 18,

327   4375–4384.

328   Oztekin, Y., Ramanaviciene, A., Ramanavicius, A., 2011. Electroanal. 23, 701−709.

329   Pacsial-Ong, E.J., McCarley, R.L., Wang, W., Strongin, R.M., 2006. Anal. Chem. 78,

330   7577–7581.

331 Paczosa-Bator, B., Pięk, M., Piech, R., 2015. Anal. Chem. 87, 1718–1725.

332 Pandey, P.C., Pandey, A.K., 2012. Analyst 137, 3306–3313.

333 Pang, H., Shi, Y., Du, J., Ma, Y., Li, G., Chen, J., Zhang, J., Zheng, H., Yuan, B.,
334   Electrochim. Acta 2012, 256–262.

335 Pereira-Rodrigues, N., Cofré, R., Zagal, J.H., Bedioui, Fethi., 2007. Bioelectrochem.
336   70, 147–154.

337 Raoof, J.B., Ojani, R., Baghayeri, M., 2009. Sens. Actuators B: Chem. 143, 261–269.

338 Rotariu, L., Zamfir, L.G., Bala, C., 2012. Anal. Chim. Acta 748, 81–88.

339 Safavi, A., Maleki, N., Farjami, E., Mahyari, F.A., 2009. Anal. Chem. 81, 7538–7543.

340 Salehzadeh, H., Nematollahi, D., 2013. Electrochim. Acta 111, 909– 915.

341 Shahmiria, M.R., Baharia, A., Karimi-Malehb, H., Hosseinzadehc, R., Mirnia, N.,
342   2013. Sens, Actuators B: Chem 177, 70–77.

343 Shayani-Jam, H., Nematollahi, D., 2010a. Chem. Commun. 46, 409–411.

344 Shayani-Jam, H., Nematollahi, D., 2011b. Electrochim. Acta 56, 9311–9316.

345 Silva, F.A.S., Silva, M.G.A., Lima, P.R., Meneghetti, M.R., Kubota, L.T., Goulart,
346   M.O.F., 2013. Biosens. Bioelectron. 50, 202–209.

347 Uhma, S., Tuyenb, N.H., Lee, J., 2011. Electrochem. Commun. 13, 677–680.

348 Valero-Ruiz, E., González-Sánchez, M.I. Batchelor-McAuley, C., Compton, R.G.,
349   2016. Analyst 141, 144–149.

350 Wang, X., Chen, X., Evans, D.G., Yang W., 2011. Sens. Actuators B: Chem. 160,
351   1444–1449.

352 Xiong, H., Jin, B., 2011. J. Electroanal.Chem. 661, 77–83.

353 Xu. H., Xiao, J., Liu, B., Griveau, S., Bedioui, F., 2015. Biosens. Bioelectron.

354   66,438–444

355 Yuan, B., Xu, C., Liu, L. Zhang, Q., Ji, S., Pi, L., Zhang, D., Huo, Q., 2013a.

356   Electrochim. Acta 104, 78–83.

357 Yuan, B., Zhang, R., Jiao, X., Li, J., Shi, H., Zhang, D., 2014. Electrochem. Commun.

358   40, 92–95.

359 Yuan, B., Zeng, X., Deng, D., Xu, C., Liu, L., Zhang, J., Gao, Y., Pang, H., 2013b.

360   Anal. Methods 5, 1779–1783.

361 Yuan, B., Zeng, X., Xu, C., Liu, L., Ma, Y., Zhang, D., Fan, Y., 2013c. Sens. Actuators

362   B: Chem. 184, 15–20.

363 Zamfir, L.G., Rotariu, L., Bala, C., 2013. Biosens. Bioelectron. 46, 61–67.

364 Zhao, L., Zhao, L., Miao, Y., Zhang, C., 2016. Electrochim. Acta 206, 86–98.

365 Zhang, D., Xu, C., Li, S., Zhang, R., Yan, H., Miao, H., Fan, Y., Yuan, B., 2014. J.

366   Electroanal. Chem. 717-718, 219–224.

367 Zhang, F., Wen, M., Cheng, M., Liu, D., Zhu, A., Tian, Y., 2010. Chem. Eur. J. 16,

368   11115–11120.

369 Zhu, Y., Murali, S., Cai, W.W., Li, X.S., Suk, J.W., Potts, J.R., Ruoff, R.S., 2010. Adv.

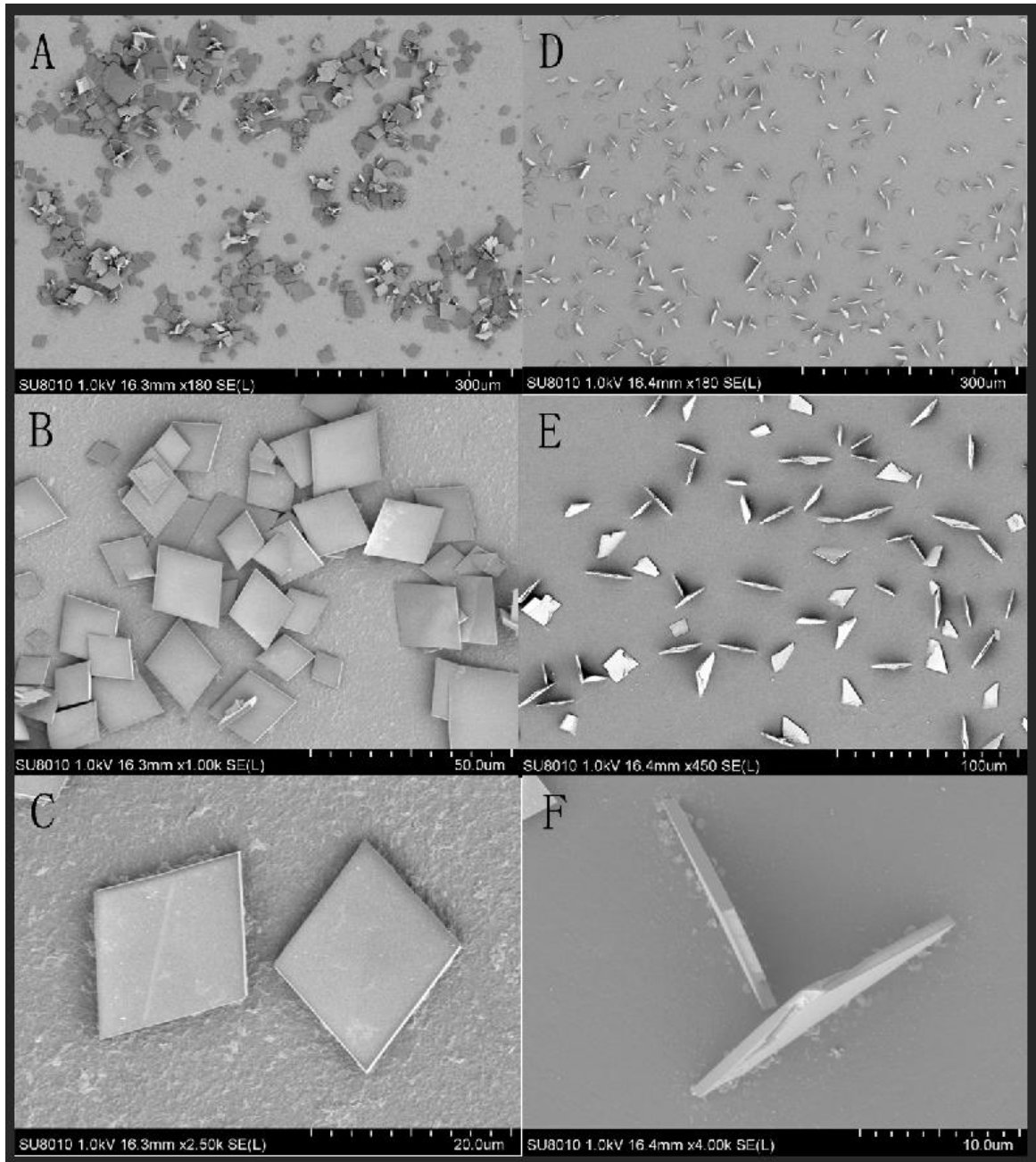370   Mater. 22, 3906–3924.

371

372

373

374

Figure captions

Fig. 1 SEM images of TCNQ/GO/GCE (A, B, and C) and TCNQ/GCE (D, E, and F) at different magnifications by a drop casting method.

Fig. 2 CVs of TCNQ/GCE (A), TCNQ/GO/GCE (B), TCNQ/rGO/GCE (C), and GO/GCE (D) in the presence (solid line, first cycle) and absence (dotted line, steady state cycle) of 5 mM GSH in 0.1 M 7.2 pH PBS at a scan rate of 0.1 V/s. *Inset* (A, B, C) first twenty cycles for corresponding electrodes.

Fig.3 CVs of TCNQ/GO/GCE in the absence (dotted line) and presence (solid line) of 0.2 mM AA (A), 5 mM CYS (B), 0.2 mM DA (C), and 0.2 mM UA (D) in 0.1 M 7.2 pH PBS at a scan rate of 0.1 V/s. *Inse*t is the CV of 5 mM GSH in the same condition.

Fig. 4 Amperometric detection of GSH by successive additions of GSH into a stirring pH 7.2 PBS solution at the TCNQ/GO/GCE at -0.05 (curve 1) and 0.1 V (curve 2). *Inset* (A): The corresponding calibration plot; (B): amplified response of the TCNQ/GO/GCE to lower concentration of GSH.

390

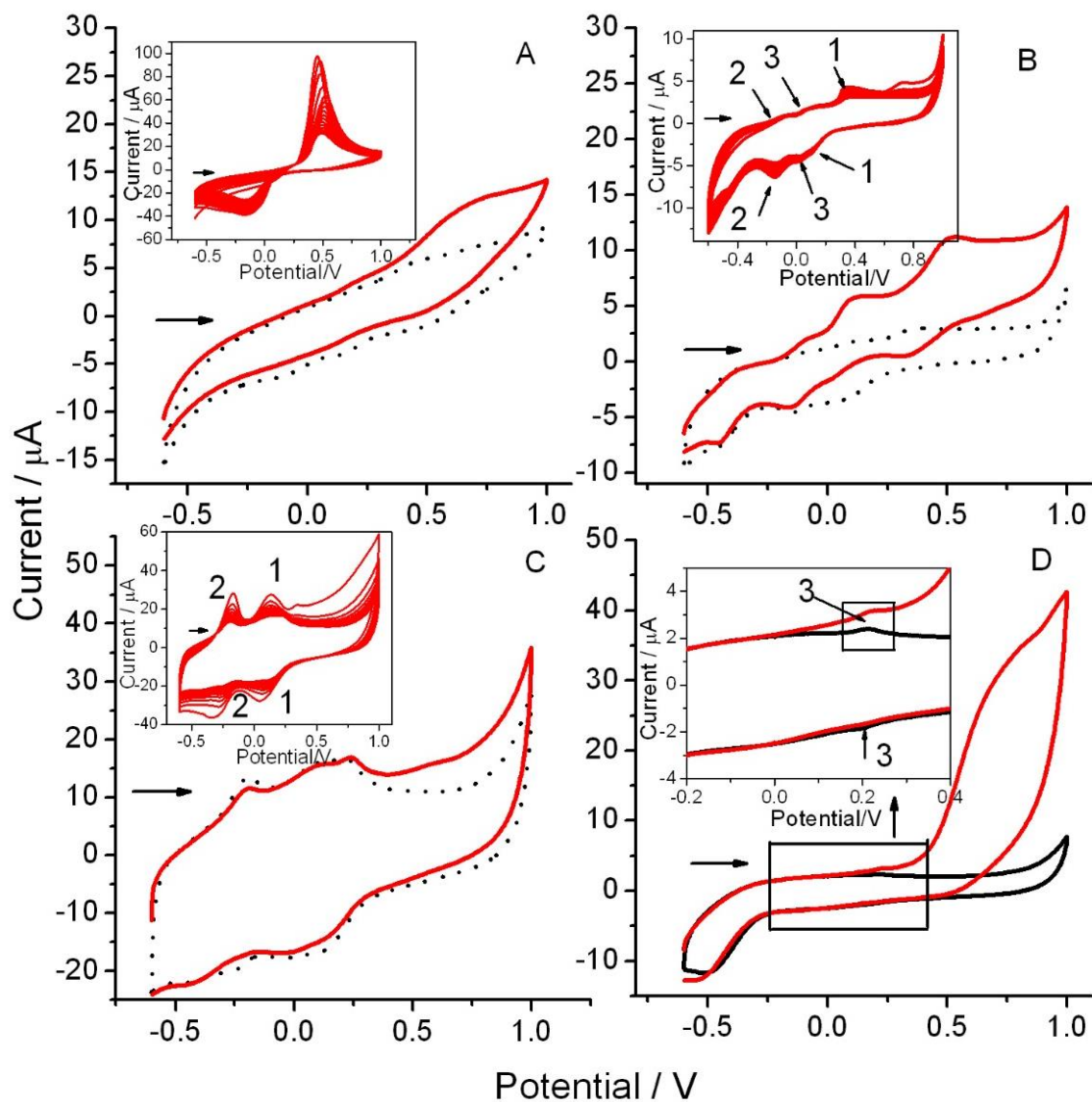Figure 1. SEM images of TCNQ/GO/GCE (A, B, and C) and TCNQ/GCE (D, E, and F) at
different magnifications by a drop casting method.

394

Figure 2. CVs of TCNQ/GCE (A), TCNQ/GO/GCE (B), TCNQ/rGO/GCE (C), and GO/GCE (D)

in the presence (solid line, first cycle) and absence (dotted line, steady state cycle) of 5 mM GSH

in 0.1 M 7.2 pH PBS at a scan rate of 0.1 V/s. *Inset* (A, B, C) first twenty cycles for corresponding

electrodes.

20

399

Figure 3. CVs of TCNQ/GO/GCE in the absence (dotted line) and presence (solid line) of 0.2 mM
AA (A), 5 mM CYS (B), 0.2 mM DA (C), and 0.2 mM UA (D) in 0.1 M 7.2 pH PBS at a scan rate
of 0.1 V/s. *Inse*t is the CV of 5 mM GSH in the same condition.

403
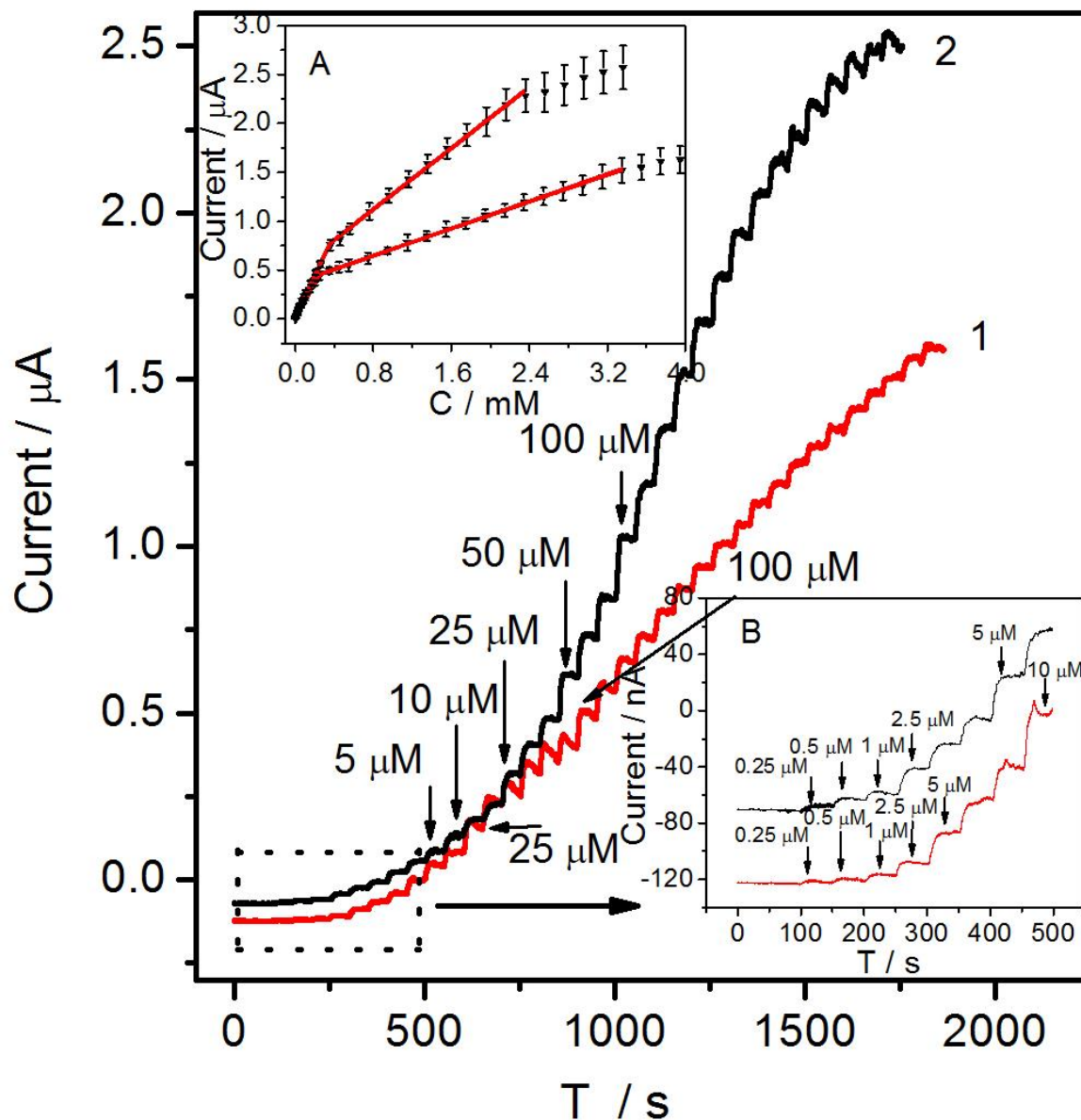
404

405　Figure 4. Amperometric detection of GSH by successive additions of GSH into a stirring pH 7.2

406　PBS solution at the TCNQ/GO/GCE at -0.05 (curve 1) and 0.1 V (curve 2). *Inset* (A): The

407　corresponding calibration plot; (B): amplified response of the TCNQ/GO/GCE to lower
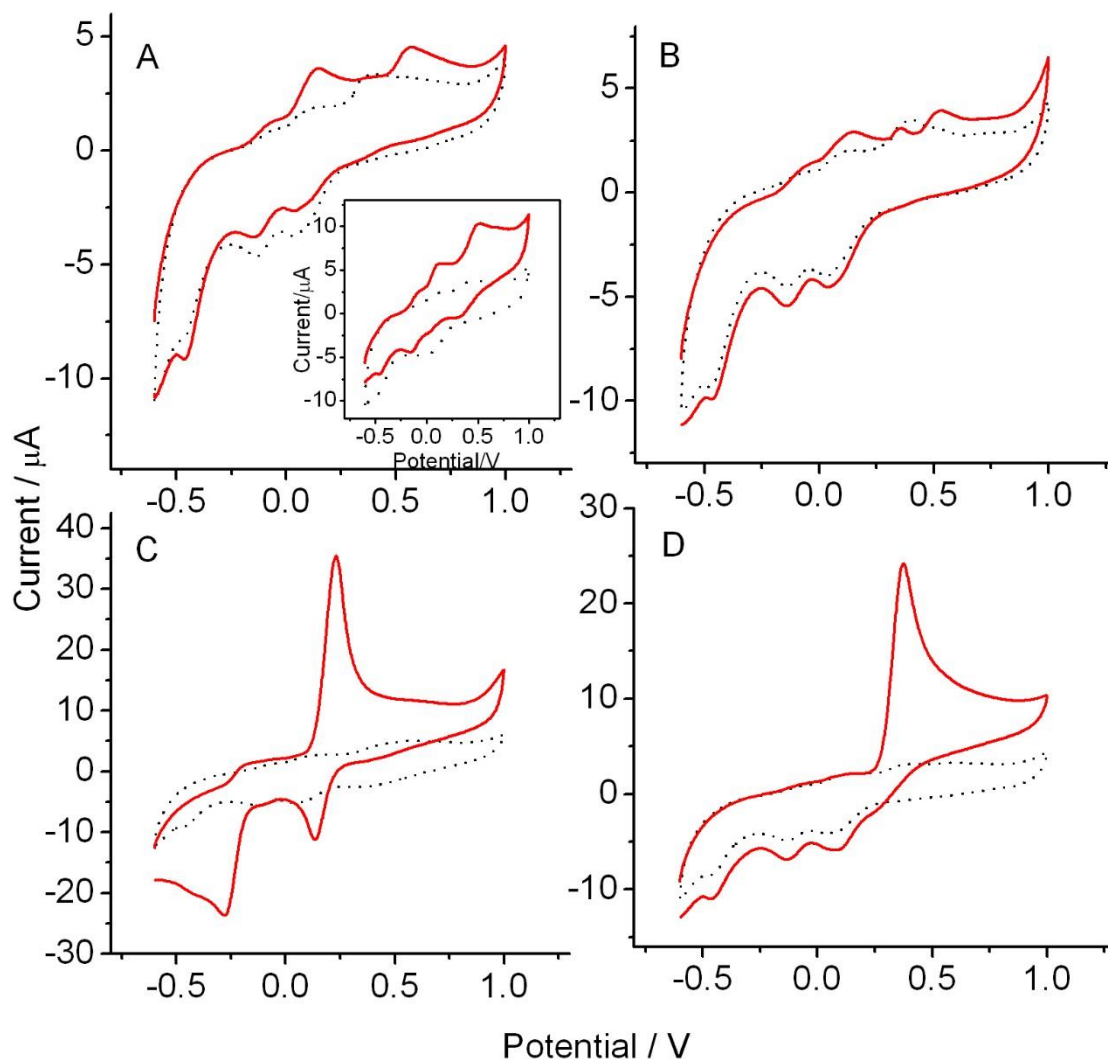
408　concentration of GSH.

409

410　**Table 1.** Analytical performances for GSH detection based on various modification

411　materials and mediators by different electrochemical methods.

Materials or mediators	Method	pH	OP/V	Linear range	LOD	References
NiO [Ml]	DPV	7.2	0.6 [a]	0.2 mM ~ 6.0 mM	0.2 mM	Chee et al., 2011

NiO microflower [Ml]	AMP	5.0	0.4 [a]	10 μM ~ 0.62 μM; 0.6 mM ~ 3.6 mM	10 μM	Pang et al., 2012
Electrodeposited NiO [Ml]	AMP	5.0	0.4 [a]	12.5 μM ~ 2.3 mM	2 μM	Yuan et al., 2013b
NiO_x/Cu_2O [Ml]	AMP	7.0	0.3 [a]	2 μM ~ 1.3 mM	0.3 μM	Yuan et al., 2013a
Poly-m-aminophenol [Ml]	AMP	4.0	0.5 [a]	0.1 μM ~ 5 μM	0.095 μM	Oztekin et al., 2011
CoPcTF [Ml]	AMP	7.4	0.18 [a]	1 μM ~ 818 μM	0.2 μM	Wang et al., 2011
CNT–SPE [Ml]	CV	7.0	0.4 [b]	10 μM ~ 100 μM	3 μM	Lee et al., 2015
MPT-HP-β-CD [Ml]	AMP	7.0	0.58 [a]	1 μM ~ 580 μM	0.87 μM	Li et al., 2015
Pd-IrO$_2$ [Ml]	AMP-CE	3.0	0.85 [a]	10 μM ~ 800 μM	2 μM	Xu et al., 2002
Electrochemical modified GO [Ml]	AMP	5.0	0.23 [a]	5 μM ~ 875 μM; 875 μM ~ 4.08 mM	5 μM	Yuan et al., 2013
Co-based metal-organic coordination polymer [Ml]	AMP	7.2	0.4 [a]	2.5 μM ~ 0.95 mM	2.5 μM	Yuan et al., 2014
NiHCF-gold [Ml]	LSV	4.0	0.65 [a]	1 μM ~1.4 mM	0.5 μM	Pandey and Pandey, 2012
Ag/CNT//polyaniline [Ml]	CV	6.0	0.4 [a]	0.3 μM ~ 3.5 mM	0.30 μM	Narang et al., 2012
Manganese dioxide [Ml]	AMP	7.5	0.45 [a]	0.5 μM ~ 10 μM	0.2 μM	Eremenko et al., 2012
Cobalt phthalocyanine [Ml]	CV	7.4	0.1 [c]	0.08 mM ~ 1 mM	~	Pereira-Rodrigues et al., 2006
Mesoporous carbon/CoO [Ml]	DPV	4.0	0.25 [a]	4 μM ~28 μM	~	Hou et al., 2009
Mesoporous carbon [Ml]	AMP	7.2	0.15 [a]	0.28 mM ~ 3 mM	~	Ndamanisha et

						al., 2009
Acetaminophen [Ml]	DPV	7.0	0.32 [c]	100 μM ~ 2.7 mM	0.37 μM	Chatraei and Zare, 2011
NiHCF/CTAB/AuNPs [Ml]	DPV	6.5	0.45 [a]	0.2 μM ~ 1 μM;	0.08 μM	He et al, 2013
Nanoscale Copper Hydroxide [Ml]	CV	7.2	0.15 [a]	1 μM ~ 50 μM; 0.1 mM ~ 1.8 mM	0.03 μM	Safavi et al., 2009
Nano-TiO$_2$/ferrocene carboxylic acid [Ml]	DPV	7.0	0.75 [a]	0.1 μM ~ 12 μM	0.098 μM	Raoof et al., 2009
NHPDA/FePt/CNT [Ml]	CV	7.0	0.41 [a]	4 nM ~ 340 μM	1 nM	Karimi-Maleh et al., 2014
Ethynylferrocene–NiO/ MWCNT [Ml]	CV	6.0	0.48 [a]	0.01 μM ~ 200 μM	6 nM	Shahmiria et al., 2013
benzamide derivative-MWCNT [Ml]	SWV	7.0	0.29 [a]	0.09 μM ~ 300 μM	0.05 μM	Ensafia et al., 2013
CoPc immobilized on nitrogen-doped graphene [Ml]	AMP	13	-0.05 [c]	1 μM ~ 8 mM	1 μM	Xu et al., 2015
Au nanoparticles [Ml]	DPV	7.4	0.33 [a]	20 μM ~ 200 μM	0.082 μM	Atta et al., 2012
CNT–ionic liquid–epinephrine [Ml]	DPV	7.0	0.28 [c]	0.1 μM ~ 30 μM	0.04 μM	Liu et al., 2015
FeT4MpyP-MWCNT [Ml]	~	7.4	0 [a]	5 μM ~ 5 mM	0.5 μM	Luz et al., 2008
FTO [Ml]	LSV	4.4	0.27 [c]	~	~	Mu and Yang, 2016
Pt-NiCo [Ml]	AMP	7.4	0 [a]	0.1 μM ~ 645 μM	0.02 μM	Zhang et al., 2010
TCNQ/GO/GCE [Ml]	AMP	7.2	-0.05 [a]	0.25 μM ~ 124.3 μM [1]	0.15 μM [1]	This work

			0.1 [a]	124.3 μM~1.67 mM [1]	0.1 μM [2]	
			0.5 [a]	0.25 μM ~ 174.3 μM [2]		
				174.3 μM-1.18 mM [2]		
I⁻/I₂ [Mr]	CV	~	0.95 [c]	19.9 μM ~ 629.4 μM;	21.28 μM	Valero-Ruiz et al., 2016
4-methylesculetin–boric acid [Mr]	CV	8.0	0.22 [a]	~	~	Salehzadeh and Nematollahi, 2013
Pyrroloquinoline Quinone [Mr]	AMP	3.5	0.50 [a]	~	13.2 μM	Inoue and Kirchhoff, 2000
4,4'-biphenol [Mr]	CV	7.0	0.35 [a]	~	~	Shayani-Jam and Nematollahi, 2011b
Acetaminophen [Mr]	CV	7.0	0.45 [a]	~	~	Shayani-Jam and Nematollahi, 2010a
Rutin [Mr]	DPV	7.0	0.27 [a]	0.5 μM ~ 25 μM	0.08 μM	Huang et al., 2015
Catechol [Mr]	CV	7.0	0.40 [b]	10 μM ~ 60 μM	3.0 μM	Lee et al., 2015
Catechol [Mr]	CV	7.4	-0.16 [a]	1 μM ~ 500 μM	0.5 μM	Zhao et al., 2016
[IrCl₆]²⁻ [Mr]	CV	7.0	0.72 [a]	~	~	Medina-Ramos et al., 2013
Catechol derivatives [Mr]	CV	7.3	0.25	~	~	Pacsial-Ong et

412 Where Ml = material; Mr = mediator; OP = oxidation potential; a = vs. Ag/AgCl electrode; b = vs.
413 Ag electrode; c = vs. Saturated Calomel Electrode; AMP = Amperometric; NHPDA =
414 N-(4-hydroxyphenyl)-3,5-dinitrobenzamide; DPV = Differential Pulse Voltammetry; LSV =
415 Linear Sweep Voltammetry; SWV = Square Wave Voltammetry; AMP-CE = Amperometric
416 method coupled with capillary electrophoresis; SPE = screen-printed electrode; MPT-HP-β-CD =
417 2-Hydroxypropyl-β-Cyclodextrin enveloped 10-methylphenothiazine; FeT4MpyP = iron(III)
418 tetra-(N-methyl-4-pyridyl)-porphyrin; FTO = fluorine doped tin oxide; ITO = indium tin oxide;
419 CoPcTF = Cobalt phthalocyaninetetrasulfonate; CNT = carbon nanotube; MWCNT =
420 multiwall carbon nanotube; NiHCF = nickel hexacyanoferrate; [1], obtained at 0 V; [2],
421 obtained at 0.1 V.
422
423
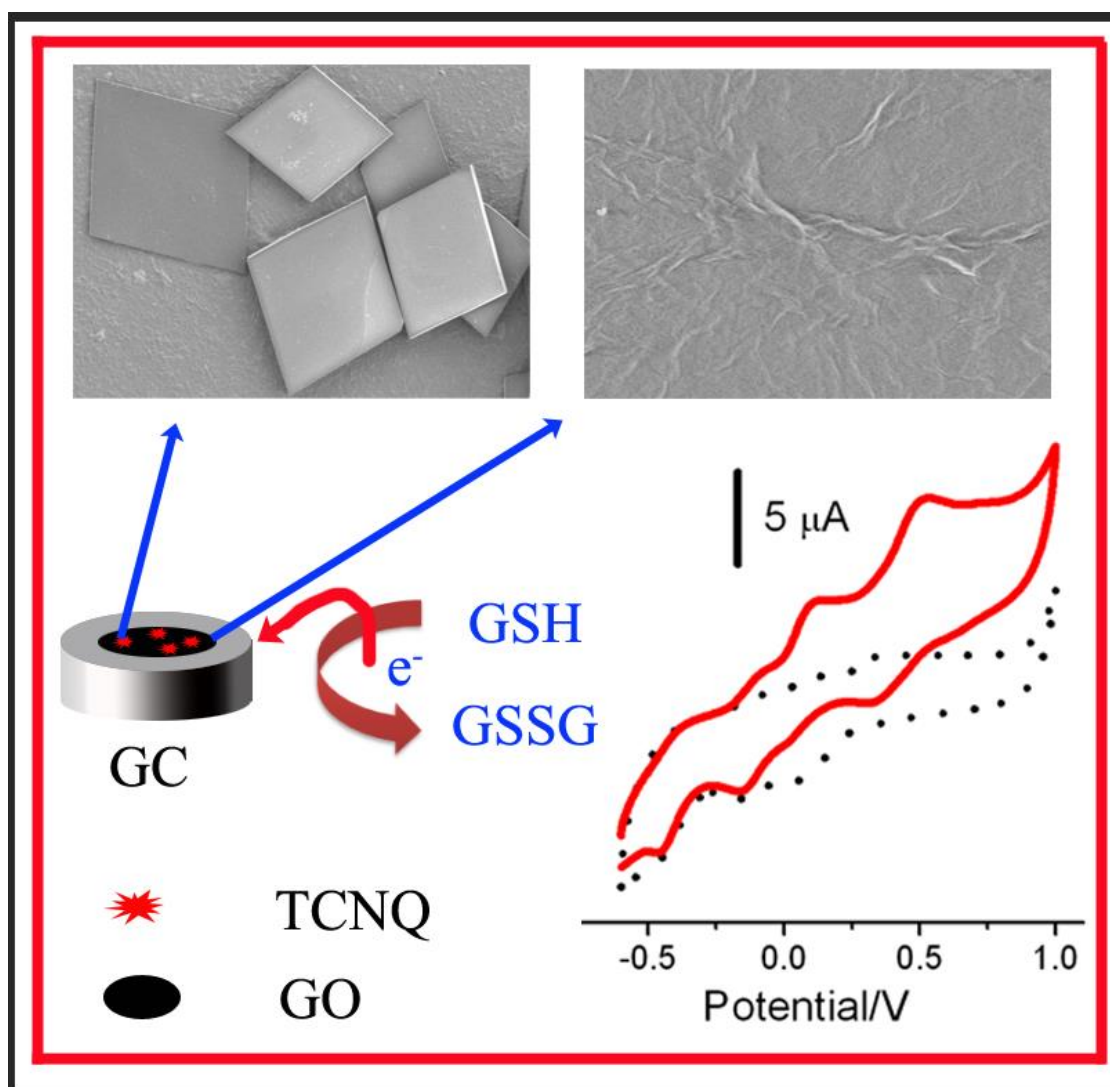
424

425 **Graphical Abstract:** TCNQ and GO modified GCE for the electrocatalytic oxidation
426 of GSH

427
428